Rapid Microwave-Assisted Deposition of Microwire Patterns of Nanoaluminum and Nanosilver from Colloids

Uğursoy Olgun*

Department of Chemistry, Faculty of Arts and Sciences, Sakarya University, Esentepe, Sakarya 54187, Turkey

ABSTRACT The rapid self-assembly of microwire patterns of 52-nm aluminum and 19-nm silver nanoparticles was demonstrated under microwave heating using novel surfactant−solvent systems. Colloid solutions of 0.03% (w/v) nanoaluminum in 10% (v/v) poly(dimethylsiloxane)−acetone were used to self-assemble the microwire patterns of Al on glass substrates, which were dipped into the solution and held against the wall. Also, colloids of 0.001% (w/v) nanosilver prepared in an acetone solution of 33.3% (v/v) chloroform, 16.6% (v/v) poly(dimethylsiloxane), and 0.3% (v/v) Tween-20 were utilized for the deposition of microwire patterns under microwave heating at 51−55 °C. The evaporation-induced self-assembly of microwire patterns at the contact line was due to stick−slip dynamics. The rapid self-assembly of micropatterns of nanoaluminum and nanosilver was also demonstrated under microwave radiation within 2 min, and the width of the microwires was about 1−20 μm depending on the concentration of nanoparticles.

KEYWORDS: microwave deposition • metal nanoparticles • self-assembly • microwire patterning • nanosilver • nanoaluminum • stick−slip motion

1. INTRODUCTION

Recently, there has been growing interest in the synthesis of nanomaterials because of their key roles in nanoelectronics (1–3), chemical sensors (4, 5), nonlinear optics (6, 7), light-emitting diodes (8, 9) and chemical catalysis (10). Also, considerable efforts have been directed toward the self-assembly of ordered arrays of nanoparticles (11). The preparation of organized patterns of nanoparticles and their processing to predictable bulk materials require new fabrication technologies. Control of the particle size, particle shape, surface functionality, and electrical conductivity is being studied for metal nanoparticles. It is also well-known that the stability, adhesion, dispersion, and reactivity properties of nanoparticles are significant during the processing of nanoparticles.

Over the past decade, micropatterned surfaces have been prepared by using photolithography (12), soft lithography (13), nanoimprint lithography (14), embossing (15), micromolding (16), and a number of other techniques (17–20). For instance, self-assembled monolayers on Au substrates have been utilized for the preparation of ceramic micropatterns from colloidal suspensions, and the resolution of micropatterns was on the order of 5 μm (21). Using self-assembled monolayers on substrate materials, approximately 5−20-μm patterns on various solid surfaces were also produced (22). The formation of TiO_2 micropatterns on Si wafers was demonstrated by using the laser direct writing method (23). In another study, the chemical etching tech-

nique was performed to prepare 5-μm patterns of a tin oxide microgas sensor (24). About 10−100-μm patterns were created using laminar flows of liquids in capillaries (25). The preparation of zeolite micropatterns and the formation of continuous ZSM-5 zeolite films at the contact line have also been studied (26–28). Other examples of patterning processes are the site-selective adhesion of hydroxyapatite microparticles (29), the fabrication of patterns of colloidal crystals on photoresist-patterned glass substrates (30), and the preparation of patterns through the selective chemical transformation of a self-assembled benzaldimine monolayer by soft X-ray irradiation (31). The micropatterning of cellular cultures on a wide range of substrates was also achieved by using the microfabricated elastomeric stencils (32). The adsorption of proteins on microfabricated surfaces has been studied for the purpose of developing microscale biosensors or biochips (33). The real-time nanosensor was also reported for the selective detection of biological and chemical species using surface functional nanowire technology (34).

The synthesis of Au and Ag nanocrystals has been studied by using various chemical routes (35–37). The light-directed assembly of Au nanoparticles was reported with a resolution of 3 μm (38). The assembly of electrically functional microwires from suspensions of Au nanoparticles was also studied by using dielectrophoretic methods (39). Micropatterns of nickel with 9-μm line widths were prepared by laser irradiation (40). The self-assembled monolayers prepared by using the photolithography technique were utilized for the fabrication of micropatterns of colloidal Au (41). Selective deposition of Ag nanoparticles by using the hydrophobic self-assembled monolayer patterns was demonstrated (42). By using colloidal dispersions in methylene chloride or chloroform, the evaporation-induced deposition of patterns of Ag
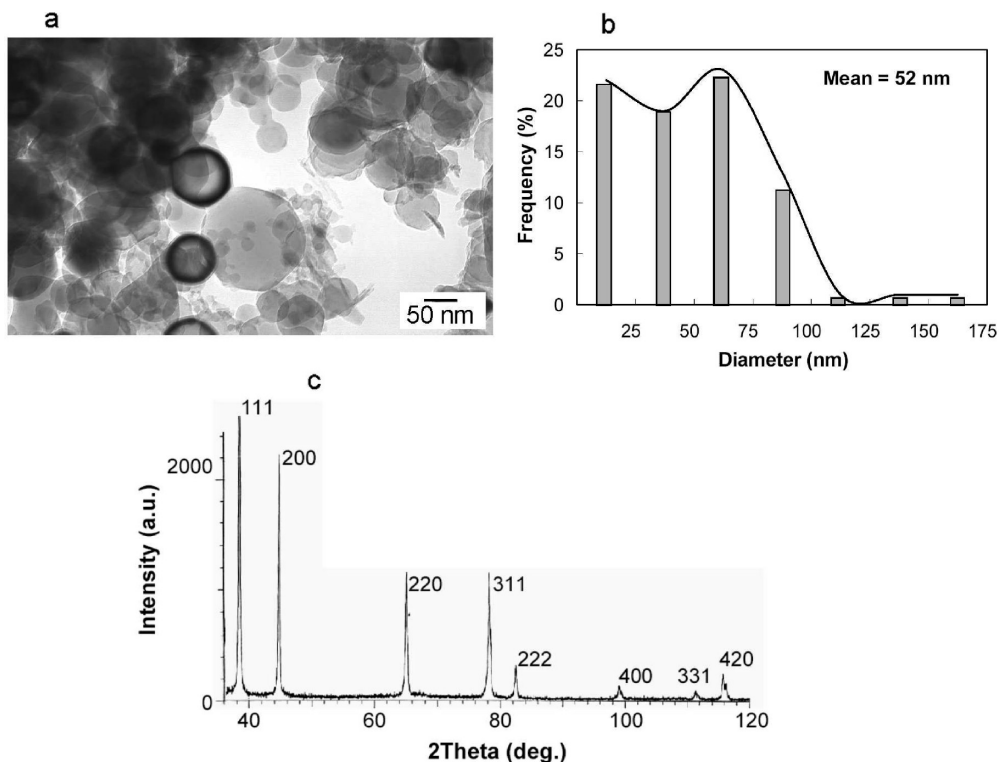
FIGURE 1. (a) TEM micrograph of Al nanoparticles utilized for the deposition of microwire patterns. (b) Particle size distribution of Al nanoparticles shown in part a. (c) Powder XRD pattern of nanoaluminum particles.

nanowires at the contact line has also been described recently (43).

The microwave-assisted self-organization of colloidal particles in confining aqueous droplets was reported for the preparation of photonic band-gap materials (44). The microwave-assisted synthesis and in situ self-assembly of coaxial Ag/C nanocables have been studied (45). Although the microwave synthesis of metal nanoparticles has been studied in the literature, the microwave processing of colloids of metal nanoparticles has not been investigated in detail. The evaporation-induced self-assembly of patterns of Ag nanowires and zeolites was reported at room temperature recently (43, 46). In this study, deposition of Al and Ag microwires was directed by the evaporation-induced self-assembly of nanoparticles under microwave heating. Compared to conventional heating, microwave radiation had many advantages, such as very short-time heating, homogeneous energy transfer to the liquid, and reduced bubble formation in solution. The formation of microwire patterns was due to stick−slip dynamics of the contact line on the surface of the substrates. By using microwave energy, the rapid self-assembly of microwires from metal nanoparticles was achieved within a few minutes for the first time.

2. EXPERIMENTAL SECTION

2.1. Preparation of Colloids. The nanoaluminum powder was obtained from Inframat. The nanoparticles were characterized by using transmission electron microscopy (TEM) and powder X-ray diffraction (XRD). The TEM micrograph shown in Figure 1a demonstrates the presence of different sized spherical Al nanoparticles. The particle size distribution graph seen in Figure 1b indicates a mean particle size of 52 nm for the nanoaluminum sample. The powder XRD pattern of nanoalu-

minum particles is also given in Figure 1c. About 10 mg of nanoaluminum powder was dispersed in 1 mL of a poly(dimethylsiloxane) (PDMS) fluid (2 cst; ABCR Inc.), and 9 mL of acetone was added into the mixture. The colloid solution was decanted with the aim of separating possibly agglomerated and large particles. The particle concentrations of nanoaluminum colloids were determined from the measurement of the turbidity at 420 nm using UV−visible spectrophotometry. The turbidity calibration graph was constructed by using the turbidity data of the standard colloids with known particle concentrations. The colloid solutions of 0.03 % (w/v) nanoaluminum in 10 % (v/v) PDMS−acetone were used for the self-asembly of microwires.

The reduction of AgNO₃ in acetone was carried out for the preparation of Ag nanoparticles. Approximately 10 mg of AgNO₃ (Merck) was stirred in 49 mL of acetone, and the mixture was heated to the boiling point before the addition of 1 mL of Tween-20 (Merck) as the reducing agent. The light-yellow solution became darker after 30 min of stirring, and a colloid of nanosilver particles was obtained. The prepared 0.01 % (w/v) Ag colloid in 2 % (v/v) Tween-20−acetone (nanosilver colloid I) was used as a stable stock solution. In a similar procedure, about 10 mg of AgNO₃ was reduced in 47 mL of acetone with rigorous stirring at room temperature in the presence of 1 mL of Tween-20 and 2 mL of PDMS. Thus, a 0.01 % (w/v) Ag colloid in an acetone solution of 4 % (v/v) PDMS and 2 % (v/v) Tween-20 (nanosilver colloid II) was prepared. With the purpose of finding a good surfactant−solvent formulation for microwire deposition from Ag nanoparticles, nanosilver colloid III was obtained by mixing 1 mL of nanosilver colloid I, 1 mL of PDMS, 2 mL of chloroform, and 2 mL of acetone. The colloid of 0.001 % (w/v) Ag prepared in an acetone solution of 33.3 % (v/v) chloroform, 16.6 % (v/v) PDMS, and 0.3 % (v/v) Tween-20 (nanosilver colloid III) was suitable for microwire deposition at room temperature and under microwave heating at 55 °C. The colloids of Ag nanoparticles were characterized by using UV−visible spectrophotometry and TEM. The UV−visible spectra of prepared Ag colloids shown in Figure 2a indicate a
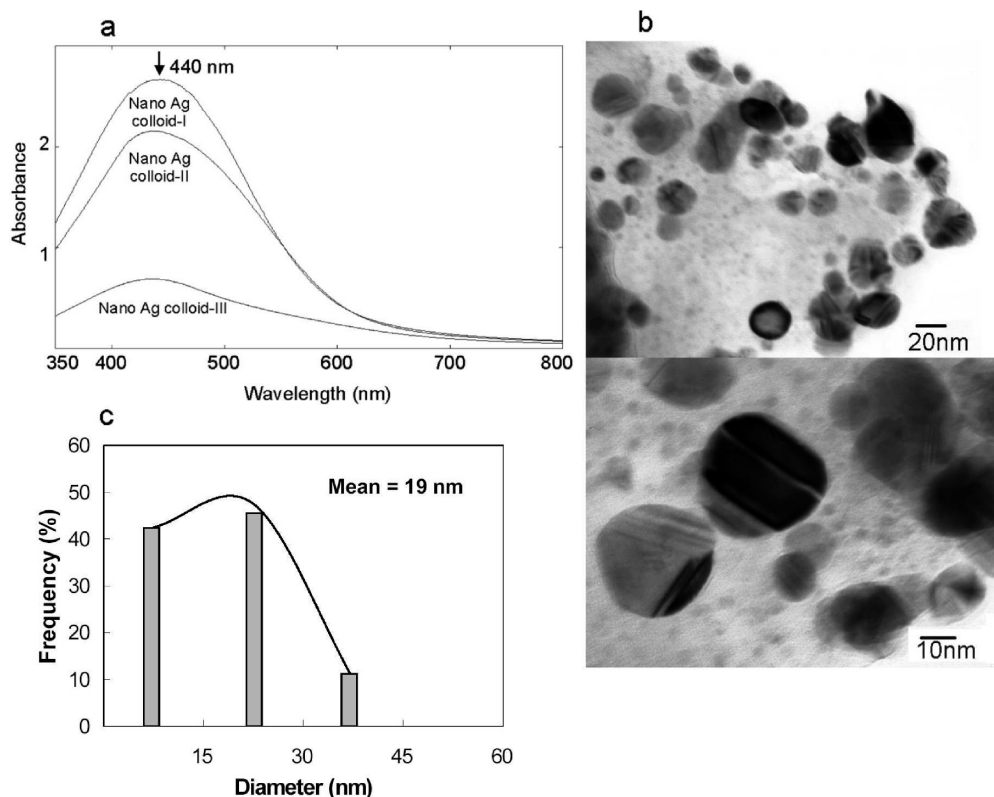
ACS APPLIED MATERIALS &INTERFACES

FIGURE 2. (a) UV−visible spectra of prepared Ag colloids showing the surface-plasmon resonance bands of Ag nanoparticles. (b) TEM micrographs of prepared Ag nanoparticles (nanosilver colloid I). (c) Histogram of the micrograph in part b demonstrating the particle size distribution of Ag nanoparticles used for the deposition of microwire patterns.
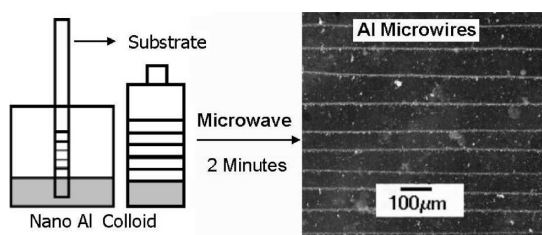

FIGURE 3. Evaporation-induced deposition of the microwire patterns under microwave heating.

maximum absorbance at 440 nm. TEM micrographs of nanosilver colloid I are also demonstrated in Figure 2b. The particle size distribution graph seen in Figure 2c indicates a mean particle size of 19 nm for the nanosilver colloid I.

2.2. Microwave-Assisted Deposition of Microwire Patterns. In this study, the formation of microwire patterns of nanoaluminum and nanosilver was carried out at a room temperature of 25 °C (the rate of acetone evaporation: 12 mg/min) and under microwave heating at 51−55 °C (the rate of acetone evaporation: 185 mg/min), as demonstrated in Figure 3. The glass substrates were prepared from the microslides (Iso Laboratory). The glass substrate was simply placed in a glass vial ($R = 20$ mm, $h = 28$ mm, and $V = 5$ mL) containing the colloid solution of nanoparticles (4 mL) and held against the wall. For the room temperature experiments, the colloid solution was kept open to air, allowing acetone to evaporate at 25 °C for 30−60 min. For microwave deposition of microwires, the colloid solution was heated at 51−55 °C for 2 min by using a microwave oven (Vestel MD-17, output 700 W, 2450 MHz). The deposition of microwires on the surface of the substrate started at the solution contact line as the solvent evaporated.

2.3. Characterization. Micrographs of Al and Ag nanoparticle were obtained by using a transmission electron microscope (JEOL JEM 3010). The powder XRD pattern of a nanoaluminum

sample was obtained by an X-ray diffractometer (Shimadzu XRD-6000). The UV−visible spectra of colloids and the turbidity measurements were recorded by a double-beam spectrophotometer (Shimadzu UV-2401 PC). The microwire patterns were studied by using an optical microscope (Motic) with a digital camera attachment. Surface characterization was also performed by a field-emission scanning electron microscope (JEOL JSM-6335F) after Au spray coating of specimens. The microscope images demonstrated the nature of prepared microwire patterns. The order of the microwire patterns, the width of the microwires, the distance between the wires, and the density of the nanoparticles were analyzed.

3. RESULTS AND DISCUSSION

3.1. Rapid Self-Assembly of Nanoaluminum Microwire Patterns. The particle deposition process is shown in Figure 3. Dispersion and stabilization of the colloids of metal particles were achieved as a result of adsorption of the surfactants and polymer chains on the surface of the particles. The selection of a suitable surfactant−solvent system was crucial to generating contact-line dynamics on the surface of the substrate. The interaction of microwave radiation with metal nanoparticles should be taken into account during rapid deposition of the microwire patterns. The rapid self-assembly of the microwire patterns of nanoaluminum under microwave radiation was carried out as shown in Figure 3. During 2 min of microwave irradiation of the colloids, the microwire patterns were generated on the surface of a flat substrate dipped into a colloid solution.
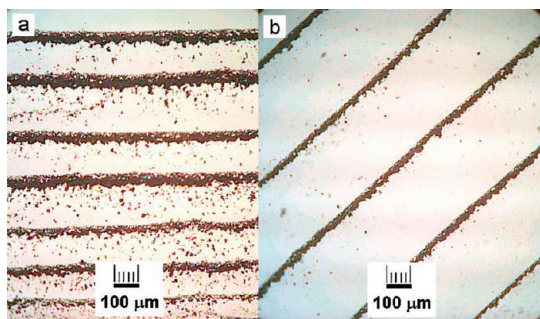
FIGURE 4. (a) Images of nanoaluminum microwires prepared from a 0.03 % (w/v) nanoaluminum colloid with 10 % (v/v) PDMS at 25 °C within 30 min. (b) Microwires of nanoaluminum deposited from a 0.03 % (w/v) nanoaluminum colloid with 10 % (v/v) PDMS under microwave heating at 51 °C within 2 min.

The colloid solutions of 0.03 % (w/v) nanoaluminum in 10 % (v/v) PDMS—acetone were used for deposition of the microwire patterns at a room temperature of 25 °C and under microwave heating at 51 °C. The microscope images of prepared microwires of nanoaluminum were presented in Figure 4. The width of the Al microwires was in the range of 20—40 μm under room temperature deposition conditions. Using microwave heating, the deposition time was reduced significantly and the width of the wires was decreased to about 10—20 μm. It was noted that, under microwave heating, the distance between microwires was increased while the width of the microwires was reduced. This was attributed to a new stick—slip pattern of the contact line due to an increase of the solution temperature. For deposition of the microwires, the typical processing time was 30—60 min at a room temperature of 25 °C and 2 min under microwave radiation.

3.2. Rapid Self-Assembly of Nanosilver Microwire Patterns.
Using deposition of smaller sized Ag particles, the width of the wire patterns was reduced significantly. The rapid self-assembly of the microwires of nanosilver was performed at a room temperature of 25 °C and under microwave heating at 51—55 °C. The solutions of nanosilver colloid I, nanosilver colloid II, and nanosilver colloid III were tested for deposition of the microwires. As expected, 0.01 % (w/v) nanosilver colloid I containing only 2 % Tween-20 exhibited complete wetting of the surface. Therefore, formation of the microwire patterns was not observed because of the lack of slip behavior. For 0.01 % (w/v) nanosilver colloid II containing 4 % (v/v) PDMS and 2 % (v/v) Tween-20, the quality of the microwires prepared at 25 °C was very low because of the disturbance of the relatively high quantity of Tween-20 in the mixture. However, deposition of the microwires was observed under microwave heating at 51 °C, as demonstrated in Figure 5. The quality of the Ag microwires was comparable with that of the microwires of nanoaluminum deposited from a 0.03 % (w/v) Al colloid. The distance between the microwires and the width of the microwires were both reduced in the case of using a 0.01 % (w/v) nanosilver colloid.

As demonstrated in Figure 6, the colloid of 0.001 % (w/v) Ag nanoparticles in a 33.3 % (v/v) chloroform—acetone mixture containing 16.6 % (v/v) PDMS and 0.3 % (v/v) Tween-
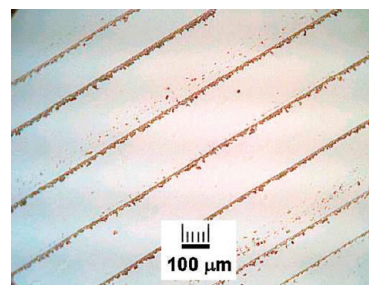
FIGURE 5. Microwire patterns of nanosilver self-assembled from 0.01 % (w/v) nanosilver colloid II under microwave heating at 51 °C within 2 min.
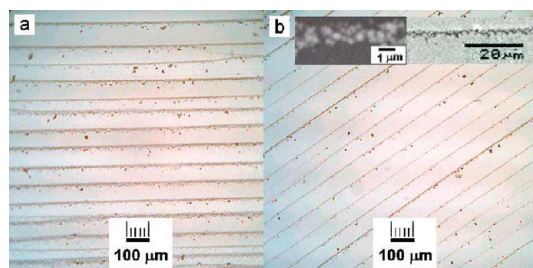
FIGURE 6. (a) Microwires of nanosilver prepared from 0.001 % (w/v) nanosilver colloid III at 25 °C within 60 min. (b) Microwires of nanosilver deposited from 0.001 % (w/v) nanosilver colloid III under microwave heating at 55 °C within 2 min.

20 (nanosilver colloid III) was suitable for the deposition of Ag microwires at 25 °C and under microwave heating at 55 °C. The quality of prepared microwires of nanosilver was excellent in terms of uniformity (no branching), and the wire patterns had long-range order. The particles were adhered to one another, and the width of the wires was as small as 1 μm under microwave heating conditions, as shown in Figure 6b. As expected, the distance between the microwires and the width of the microwires were both decreased for low concentrations of smaller size Ag nanoparticles in colloid solutions. However, it is not clear if this is a particle size effect because the nature of the particles and the solvent compositions of the colloid solutions are different compared to those of the nanoaluminum colloids. The small width of the microwire patterns is probably due to the reduced stick time of the contact line during particle deposition. The stick time is also related to the contact angle, the particle concentration, and the viscosity of the colloid at the contact line. As shown in Figure 6b, more than 20 microwires of nanosilver were deposited on the surface of the glass substrate within 2 min of the microwave treatment.

Here, the microwave-assisted particle deposition process was not limited to one particular material type or specific particle size. Nanoaluminum was obtained as a dry powder, and the surface of the particles was free of any organic capping agents. The Al sample consisted of agglomerates of many particles (Figure 1a). Thus, the colloids of Al were prepared in a predetermined surfactant—solvent system. On the other hand, the Ag colloid was produced inside the surfactant—solvent system with a reducing agent and a stabilizer. Thus, unlike Al particles, Ag nanoparticles were well-dispersed inside the colloid solution without the formation of a large number of agglomerates (Figure 1b).
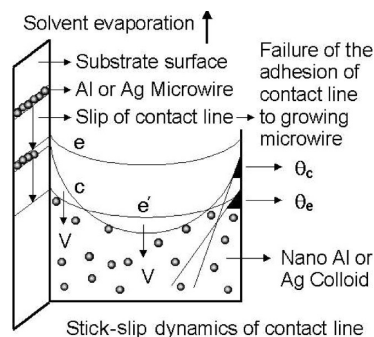
FIGURE 7. Proposed mechanism of microwire deposition demonstrated by stick—slip dynamics of the contact line.
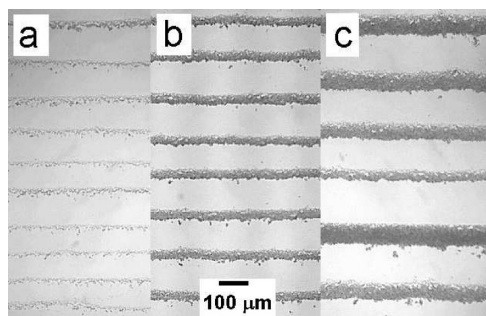

FIGURE 8. Microwire patterns prepared using 0.03% (w/v) nanoaluminum colloids with (a) 5%, (b) 10%, and (c) 20% PDMS in acetone.

3.3. Stick—Slip Dynamics of the Contact Line.

The mechanism of particle deposition and stick—slip dynamics of the contact line are demonstrated in Figure 7. Initially, the contact line sticks to the wall surface with a contact angle of θ_e (about 20—25°) at position e during the evaporation process. After deposition of the nanoparticles at the contact line, the meniscus reaches a critical point with an estimated contact angle of θ_c (about 16—18°) at position c. The instantaneous slip of the contact line from position c to e' is due to contraction of the colloid solution from the wall surface into the center. At this critical position, the cohesive force in the perpendicular direction is greater than the adhesive force at the wall because of the reduced contact angle ($\cos \theta_c > \cos \theta_e$). Therefore, the contact line of the colloid solution slips on the surface of the substrate because of failure of adhesion of the contact line to the growing microwire. The possible adsorption of PDMS, together with the particles at the contact line, may also play a role in stick—slip dynamics. The mechanism of microwire formation and stick—slip dynamics have been explained previously (19, 43, 46). The works of Deegan et al. indicated that deposition of the particles at the contact line is a general phenomenon with only three requirements (47–49). First, the solvent has a nonzero contact angle (partially wettable). Second, the solvent can evaporate. Third, the contact line can be pinned (stick—slip behavior). In conclusion, deposition of the nanoparticles is due to stick—slip dynamics of the three-phase contact line of the colloid solutions during evaporation of the solvent.

3.4. Effect of PDMS on Microwire Patterns.

The use of PDMS as a surfactant in metal colloids enhanced the deposition of the particles at the contact line during solvent
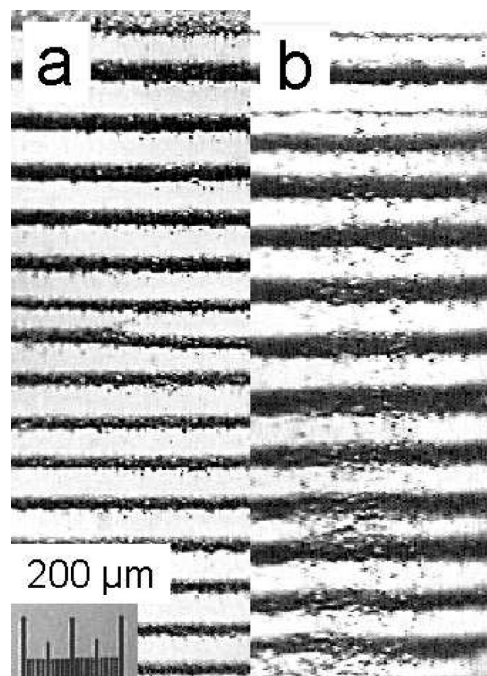

FIGURE 9. Microwire patterns of nanoaluminum prepared from a 0.03% (w/v) nanoaluminum colloid with 10% (v/v) PDMS at (a) 20 °C and (b) 40 °C using conventional heating.
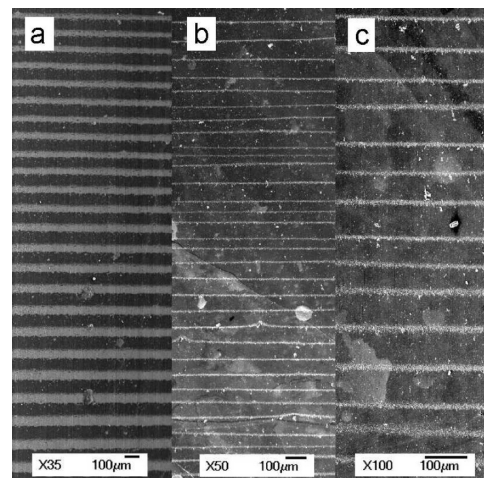

FIGURE 10. Microwires of nanoaluminum prepared from a 0.03% (w/v) nanoaluminum colloid with 10% (v/v) PDMS at (a) 20 °C and (b and c) 55 °C using microwave heating.

evaporation. On the other hand, Tween-20 is a well-known hydrophilic surfactant and provides a complete wetting of the contact line by the colloids (the contact angle is zero, $\theta = 0°$). Therefore, deposition of the particles was not observed in the presence of only Tween-20. As it was also demonstrated in our previous work, the presence of a hydrophobic PDMS-type surfactant in colloid solutions promotes particle deposition at the contact line (the contact angle is not zero, $\theta > 0°$) (46). Also, the metal—PDMS interface was simulated using the molecular dynamics method (50). It was demonstrated that the PDMS—Fe interface has an adhesive energy of -68 cal/cm^3 while the cohesive energy of PDMS is -61 cal/cm^3. The distance of the observed Si—CH$_3$···OH—Fe hydrogen bond was pre-

Table 1. Effect of Microwave Heating on Deposition of the Microwire Patterns of Nanoaluminum Particles: 230 × 114 mm (96 × 96 DPI)

method of particle deposition	parameters for nanoaluminum microwire patterns					
	deposition time (s)	no. of produced microwires	rate of evaporation (kg/m^2 · s)	stick time (s)	microwire spacing (μm)	microwire width (μm)
microwave heating (55 °C)	120	35	$(10-24) \times 10^{-3}$	3.4	50−60	10
conventional heating (40 °C)	1200	14	$(1.5-2) \times 10^{-3}$	86	60−70	40−60
room temperature (20 °C)	3600	19	$(0.3-0.8) \times 10^{-3}$	190	60−70	25−50

dicted as 2.786 Å. Similar interactions were estimated for both the nanoaluminum−PDMS and nanosilver−PDMS interfaces in colloids. The possible effects of increasing concentrations of PDMS on the deposition of microwire patterns were studied using 0.03 % (w/v) nanoaluminum colloids with 5 %, 10 %, and 20 % PDMS in acetone. The results demonstrated in Figure 8 clearly indicated that higher concentrations of PDMS increase both the width of the microwires and the spacing between the microwires.

3.5. Effect of Microwave Heating on Microwire Deposition.
The contact-line deposition of nanoparticles has been studied by several groups to prepare microwires of various materials (43, 51, 52). They used Ag nanowires in methylene chloride, a benzothiophene derivative in *p*-xylene, and poly(2-methoxy-5-(2-ethylhexyloxy)-1,4-phenylenevinylene) solutions in toluene for deposition of the micropatterns. In this study, the effects of using microwave heating were explored for the first time to accelerate the particle deposition process. The role of microwaves during the stick−slip motion of the contact line was investigated using the colloids of nanoaluminum particles. The colloid solutions of 0.03 % (w/v) nanoaluminum (4 mL) containing 10 % (v/v) PDMS were placed in glass vials (with a radius of 12 mm), and deposition of the microwires on the wall surface was carried out at 20 °C without heating, at 40 °C with conventional heating, and at 55 °C with microwave heating. As demonstrated in Figures 9 and 10, the microwire patterns produced using the conventional heating source and the microwave are very different compared to those for deposition of the Al nanoparticles at room temperature. Under conventional heating at 40 °C, the width of the wire patterns is increased from 25 to 50 μm, but the distance between the microwires remains almost the same (60−70 μm). On the other hand, under microwave heating at 55 °C, the width of the microwire patterns is reduced to about 10 μm and the spacing is also decreased to 50−60 μm. Also, the surface microstructure of the microwire patterns is different, as shown in Figure 9b for conventional heating and in Figure 10b,c for microwave heating. The effects of microwave heating on deposition of the microwire patterns of nanoaluminum particles are summarized in Table 1. It was demonstrated that the microwire patterns produced under microwave heating have smaller wire widths compared to those of the micropatterns prepared using conventional self-assembly processes. The same effect was also observed for the microwires of nanosilver particles, as shown in Figure 6b. The results clearly demonstrated that

both the processing time of pattern formation and the width of the microwires are reduced significantly using microwave heating.

The spacing of the microwire patterns (*Y*) is dependent on the contact angle (θ), the pinning height (*h*), and the particle diameter (*D*), as expressed by the following equation (53):

$$Y = (D - h)/\tan \theta \quad (1)$$

The width of the microwires, X_0, can be related to the stick time of *t* by using the following equation as suggested by Rio et al. (54):

$$X_0 \propto t^{2/3} \Phi *^{-2/3} \quad (2)$$

where $\Phi^* = (\Phi_c/\Phi_0)^{3/4} - 1$, which Φ_0 is the initial particle concentration at the contact line and Φ_c is the critical particle concentration at the contact line for the stick time of *t*. Equation 2 is used to describe the particle deposition at advancing contact line. However, in this study, deposition of the particles was produced at a receding contact line during microwave heating. Nevertheless, the width of the deposited microwires was increased as a function of the stick time, as demonstrated by the experimental results presented in Table 1. Other parameters, such as the temperature, particle size, surfactant concentration, substrate type, particle−particle interaction, and particle−substrate adhesion, should also be taken into account. For example, the effect of the particle size on the width of the deposited patterns was studied by Stebe et al. (55). Their results showed that both the width of the patterns and the spacing are sensitive to the particle size.

The evaporation-induced deposition of micropatterns of Ag nanowires (43) and the formation of patterns from dilute polymer solutions without any particles (56) have been reported recently. The growth of electrically conductive microwires from Au nanoparticle suspensions (39) and the deposition of metallic nanowires of Pd between microelectrodes have been carried out using aqueous solutions (57, 58). In these studies, a single wire or a small number of wires with branched structures were grown unless the gap sizes of the electrodes were reduced to 10−15 μm (57). Electrodeposition of copper wire arrays (59), the magnetic-field-directed growth of CoPt$_3$ nanocrystal microwires (60), and electroless deposition of Ag metal directly on the exposed, developed photographic film (61) were also reported. However, most of these deposition processes are time-consuming and they are not very effective for simultaneous deposition on multiple substrates during the mass production of such microwires.

4. CONCLUSIONS

In this study, the evaporation-induced rapid self-assembly of the microwires of nanoaluminum and nanosilver has been demonstrated under microwave heating by using different surfactant−solvent formulations. Deposition of the microwires at the contact line was due to stick−slip dynamics. The results showed that, under microwave heating, the PDMS−acetone system was adequate for the formation of microwires of nanoaluminum. The experimental results also indicated that the use of PDMS and Tween-20 in acetone or an acetone−chloroform mixture was essential for deposition of the microwires of nanosilver under microwave heating. The width of the microwires was typically 1−20 μm, and the distance between the microwires was about 50−300 μm. Using microwave processing of the nanoparticles, the width of the microwires and the distance between the microwires were both decreased. PDMS was used for the purpose of promoting microwire deposition, while Tween-20 was added as a stabilizer for Ag nanoparticles to prevent further agglomeration and growth in solution. The microwire deposition process presented in this study is relatively simple compared to the previous patterning techniques. The use of a photoresist layer, a micropatterned mask, a monolayer coating, and molded patterns is not required. As a result of these findings, it was concluded that the colloids of Al and Ag nanoparticles are suitable for the rapid self-assembly of microwire patterns under microwave heating. The rapid self-organization of nanoparticles is highly desirable, especially for the large-scale fabrication of nanowire devices.

Supporting Information Available: Movie file demonstrating the evaporation-induced self-assembly of nanoaluminum particles at the contact line during stick−slip motion. This material is available free of charge via the Internet at http://pubs.acs.org.

REFERENCES AND NOTES

(1) Lu, W.; Lieber, C. M. *Nat. Mater.* **2007**, *6*, 841.
(2) Ferry, D. K. *Science* **2008**, *319*, 579.
(3) Brongersma, M. L.; Zia, R.; Schuller, J. A. *Appl. Phys. A: Mater. Sci. Process.* **2007**, *89*, 221.
(4) Homola, J. *Chem. Rev.* **2008**, *108*, 462.
(5) Haick, H. *J. Phys. D* **2007**, *40*, 7173.
(6) Newman, D. M.; Wears, M. L.; Matelon, R. J.; McHugh, D. *Appl. Phys. B: Lasers Opt.* **2002**, *74*, 719.
(7) Zong, R.; Zhou, J.; Li, Q.; Li, L.; Wang, W.; Chen, Z. *Chem. Phys. Lett.* **2004**, *398*, 224.
(8) Butun, B.; Cesario, J.; Enoch, S.; Quidant, R.; Ozbay, E. *Photonics Nanostruct.* **2007**, *5*, 86.
(9) Huang, H. W.; Kuo, H. C.; Chu, J. T.; Lai, C. F.; Kao, C. C.; Lu, T. C.; Wang, S. C.; Tsai, R. J.; Yu, C. C.; Lin, C. F. *Nanotechnology* **2006**, *17*, 2998.
(10) Fan, J.; Gao, Y. *J. Exp. Nanosci.* **2006**, *1*, 457.
(11) Shipway, A. N.; Katz, E.; Willner, I. *ChemPhysChem* **2000**, *1*, 18.
(12) Gorzolnik, B.; Mela, P.; Moeller, M. *Nanotechnology* **2006**, *17*, 5027.
(13) Zhang, S.; Wang, Q.; Zhang, X.; Wang, Y.; Li, L.; Wang, L.; Chen, J. *Laser Phys. Lett.* **2008**, *5*, 59.
(14) Garrett, D. J.; Lehr, J.; Miskelly, G. M.; Downard, A. J. *J. Am. Chem. Soc.* **2007**, *129*, 15456.
(15) Hong, S. H.; Lee, J. H.; Lee, H. *Microelectron. Eng.* **2007**, *84*, 977.
(16) Park, J. H.; Choi, S. O.; Kamath, R.; Yoon, Y. K.; Allen, M. G.; Prausnitz, M. R. *Biomed. Microdevices* **2007**, *9*, 223.
(17) Innocenzi, P.; Kidchob, T.; Falcaro, P.; Takahashi, M. *Chem. Mater.* **2008**, *20*, 607.
(18) Wang, J.; Stover, H. D. H.; Hitchcock, A. P. *J. Phys. Chem. C* **2007**, *111*, 16330.
(19) Prevo, B. G.; Kuncicky, D. M.; Velev, O. D. *Colloids Surf., A* **2007**, *311*, 2.
(20) Sun, W. Q.; Lam, K. F.; Wong, L. W.; Yeung, K. L. *Chem. Commun.* **2005**, *39*, 4911.
(21) Heule, M.; Schönholzer, U. P.; Gauckler, L. J. *J. Eur. Ceram. Soc.* **2004**, *24*, 2733.
(22) Sugimura, H.; Hozumi, A.; Kameyama, T.; Takai, O. *Adv. Mater.* **2001**, *13*, 667.
(23) Kordás, K.; Pap, A. E.; Leppävuori, S. *Surf. Coat. Technol.* **2003**, *176*, 84.
(24) Chung, W. Y.; Lim, J. W. *Curr. Appl. Phys.* **2003**, *3*, 413.
(25) Takayama, S.; Ostuni, E.; Qian, X.; McDonald, J. C.; Jiang, X.; LeDuc, P.; Wu, M. H.; Ingber, D. E.; Whitesides, G. M. *Adv. Mater.* **2001**, *13*, 570.
(26) Ha, K.; Lee, Y. J.; Jung, D. Y.; Lee, J. H.; Yoon, K. B. *Adv. Mater.* **2000**, *12*, 1614.
(27) Ha, K.; Lee, Y. J.; Chun, Y. S.; Park, Y. S.; Lee, G. S.; Yoon, K. B. *Adv. Mater.* **2001**, *13*, 594.
(28) Jung, K. T.; Shul, Y. G. *J. Membr. Sci.* **2001**, *191*, 189.
(29) Zhu, P. X.; Masuda, Y.; Koumoto, K. *J. Colloid Interface Sci.* **2001**, *243*, 31.
(30) Li, J.; Xing, R.; Huang, W.; Han, Y. *Colloids Surf., A* **2005**, *269*, 22.
(31) Jung, Y. J.; Kim, J. I.; Kang, T. H.; Ihm, K.; Kim, K. J.; Kim, B.; Park, J. W. *J. Colloid Interface Sci.* **2005**, *282*, 241.
(32) Folch, A.; Jo, B. H.; Hurtado, O.; Beebe, D. J.; Toner, M. *J. Biomed. Mater. Res.* **2000**, *52*, 346.
(33) Bashir, R.; Gomez, R.; Sarikaya, A.; Ladisch, M. R.; Sturgis, J.; Robinson, J. P. *Biotechnol. Bioeng.* **2001**, *73*, 324.
(34) Cui, Y.; Wei, Q.; Park, H.; Lieber, C. M. *Science* **2001**, *293*, 1289.
(35) Raveendran, P.; Fu, J.; Wallen, S. L. *J. Am. Chem. Soc.* **2003**, *125*, 13940.
(36) Jana, N. R.; Peng, X. *J. Am. Chem. Soc.* **2003**, *125*, 14280.
(37) Volpe, M. V.; Longo, A.; Pasquini, L.; Casuscelli, V.; Carotenuto, G. *J. Mater. Sci. Lett.* **2003**, *22*, 1697.
(38) Vossmeyer, T.; DeIonno, E.; Heath, J. R. *Angew. Chem., Int. Ed. Engl.* **1997**, *36*, 1080.
(39) Hermanson, K. D.; Lumsdon, S. O.; Williams, J. P.; Kaler, E. W.; Velev, O. D. *Science* **2001**, *294*, 1082.
(40) Kikuchi, T.; Sakairi, M.; Takahashi, H.; Abe, Y.; Katayama, N. *Surf. Coat. Technol.* **2003**, *199*, 169.
(41) Liu, J. F.; Zhang, L. G.; Gu, N.; Ren, J. Y.; Wu, Y. P.; Lu, Z. H.; Mao, P. S.; Chen, D. Y. *Thin Solid Films* **1998**, *176*, 327.
(42) Yang, K. Y.; Kim, J. W.; Byeon, K. J.; Lee, H. *Microelectron. Eng.* **2007**, *84*, 1552.
(43) Huang, J.; Fan, R.; Connor, S.; Yang, P. *Angew. Chem., Int. Ed.* **2007**, *46*, 2414.
(44) Kim, S. H.; Lee, S. Y.; Yi, G. R.; Pine, D. J.; Yang, S. M. *J. Am. Chem. Soc.* **2006**, *128*, 10897.
(45) Yu, J. C.; Hu, X. L.; Quan, L. B.; Zhang, L. Z. *Chem. Commun.* **2005**, *21*, 2704.
(46) Olgun, U.; Sevinç, V. *Powder Tech.* **2008**, *183*, 207.
(47) Deegan, R. D.; Bakajin, O.; Dupont, T. F.; Huber, G.; Nagel, S. R.; Witten, T. A. *Nature* **1997**, *389*, 827.
(48) Deegan, R. D.; Bakajin, O.; Dupont, T. F.; Huber, G.; Nagel, S. R.; Witten, T. A. *Phys. Rev. E* **2000**, *62*, 756.
(49) Deegan, R. D. *Phys. Rev. E* **2000**, *61*, 475.
(50) Olgun, U.; Kalyon, D. M. *Polymer* **2005**, *46*, 9423.
(51) Liu, N.; Zhou, Y.; Wang, L.; Peng, J.; Wang, J.; Pei, J.; Cao, Y. *Langmuir* **2009**, *25*, 665.
(52) Hong, S. W.; Byun, M.; Lin, Z. *Angew. Chem., Int. Ed.* **2009**, *48*, 512.
(53) Ray, M. A.; Kim, H.; Jia, L. *Langmuir* **2005**, *21*, 4786.
(54) Rio, E.; Daerr, A.; Lequeux, F.; Limat, L. *Langmuir* **2006**, *22*, 3186.
(55) Ghosh, M.; Fan, F.; Stebe, K. J. *Langmuir* **2007**, *23*, 2180.
(56) Yabu, H.; Shimomura, M. *Adv. Funct. Mater.* **2005**, *15*, 575.
(57) Cheng, C.; Gonela, R. K.; Gu, Q.; Haynie, D. T. *Nano Lett.* **2005**, *5*, 175.
(58) Ranjan, N.; Vinzelberg, H.; Mertig, M. *Small* **2006**, *2*, 1490.
(59) Zhang, M.; Zuo, G.; Zong, Z.; Chen, H.; He, Z.; Yang, C.; Li, D.; Zou, G. *Appl. Phys. Lett.* **2006**, *88*, 203106.
(60) Beecher, P.; Shevchenko, E. V.; Weller, H.; Quinn, A. J.; Redmond, G. *Adv. Mater.* **2005**, *17*, 1080.
(61) Deng, T.; Arias, F.; Ismagilov, R. F.; Kenis, P. J. A.; Whitesides, G. M. *Anal. Chem.* **2000**, *72*, 645.